Colloid Polym Sci (2004) 282: 833–843
DOI 10.1007/s00396-004-1131-2

ORIGINAL CONTRIBUTION

Tune B. Bonné
Karin Lüdtke
Rainer Jordan
Petr Štěpánek
Christine M. Papadakis

Aggregation behavior of amphiphilic poly(2-alkyl-2-oxazoline) diblock copolymers in aqueous solution studied by fluorescence correlation spectroscopy

Received: 5 February 2004
Accepted: 5 April 2004
Published online: 7 May 2004

Dedicated to Prof. Dr. Erhard W. Fischer on the occasion of his 75th birthday

T. B. Bonné · C. M. Papadakis (✉)
Fakultät für Physik und Geowissenschaften, Universität Leipzig, Linnéstr. 5, 04103 Leipzig, Germany
E-mail: Christine.Papadakis@ph.tum.de

K. Lüdtke · R. Jordan
Chemie Department, Technische Universität München, Lichtenbergstr. 4, 85747 Garching, Germany

P. Štěpánek
Institute of Macromolecular Chemistry, Academy of Sciences of the Czech Republic, Heyrovsky Sq. 2, CZ-16206 Prague, Czech Republic

Present address: T. B. Bonné
C. M. Papadakis
Physik Department E13, Technische Universität München, James-Franck-Str. 1, 85747 Garching, Germany

R. Jordan
Department of Chemistry, Chemical Engineering and Materials Science, Polytechnic University, Six Metrotech Center, Brooklyn NY 11201, USA

Abstract The diffusional behavior of amphiphilic poly(2-oxazoline) diblock copolymers in aqueous solution is studied using photon correlation spectroscopy (PCS) and fluorescence correlation spectroscopy (FCS). The polymers were synthesized by living cationic polymerization and were fluorescence-labeled with tetramethyl rhodamine isothiocyanate either at the end of the hydrophilic or the hydrophobic block. Temperature-resolved PCS showed that, at room temperature, large metastable aggregates are present along with unimers and micelles. An annealing above ~40 °C resulted in stable equilibrium micellar solutions. By means of FCS, the hydrodynamic radii of the unimers and the micelles were measured simultaneously in a broad concentration range, and the critical micelle concentration could be determined. Comparison of the results from conventional PCS measurements with this first FCS study showed excellent agreement and the high potential of the FCS technique.

Keywords Self-diffusion · Fluorescence correlation spectroscopy · Amphiphilic diblock copolymers · Polysoaps · Micelle formation

Introduction

In aqueous solution, amphiphilic block copolymers spontaneously aggregate into micellar solutions and complex lyotropic phases, which are reminiscent of the structures encountered in low molar mass surfactants or lipids. Their phase behavior as well as the characteristics and the formation of micelles have been extensively studied [1–9].

A number of anionically synthesized—thus structurally defined—amphiphilic diblock copolymers have been studied in aqueous solution, such as various poly[(olefin)-*b*-(ethyleneoxide)] type diblock copolymers [10 – 17] as well as various poly[(ethyleneoxide)-*b*-(oxy butylene)] diblock copolymers and a poly[(oxyphenylethylene)-*b*-(ethyleneoxide)] diblock copolymer [18]. Most of the systems studied feature the ethyleneoxide block as the hydrophilic moiety.

Poly(2-oxazoline) block copolymers—the system presented here—constitute a versatile system to systematically study the aggregation behavior and correlate it to the polymer architectural features. In contrast to the popular Pluronics-type amphiphiles (poly[(ethyleneoxide)(propyleneoxide)(ethyleneoxide)], PEO-PPO-PEO), the architecture and the degree of hydrophobicity of the blocks can be controlled, and additional functionalizations can be introduced in the polymer sidechains as well as at the chain termini. The amphiphilic contrast can be adjusted by the block copolymerization of two or more 2-alkyl-2-oxazoline monomers where 2-methyl- and 2-ethyl-2-oxazolines are hydrophilic, whereas side groups longer than propyl result in increasing hydrophobicity [19]. The amphiphilic motif is given both by the composition of the two blocks (e.g., poly[(2-*n*-nonyl-2-oxazoline)-*b*-(2-methyl-2-oxazoline)]) (a non-ionic amphiphile) as well as within each monomer unit composed of a hydrophilic amide group and a hydrophobic alkyl side chain, thus being an amphiphile by itself (a non-ionic polysoap). The synthesis by means of living cationic polymerization enables the realization of a vast variety of structural options such as homopolymers, diblock and triblock copolymers, stars, dendrimers, hyperbranched polymers, and lipopolymers [20 – 23].

The possibilities of a site-selective introduction of fluorescence labels are of great importance for correlating the observed physical properties of the supramolecular aggregates with the specific polymer architecture. Such functional and structural variety as well as the fine-tuning of the hydrophilic lipophilic balance (HLB) and the molecular packing geometry within the resulting assemblies is not realizable in PEO-PPO systems.

Poly(2-oxazoline)s contain the amide motif which is also present in other biocompatible polymers, e.g., poly(*N*-vinylpyrolidone), and can also be found in peptides and proteins. Water-soluble poly(2-oxazoline)s were found to be non-toxic, and immuno-response has not been reported even in complex biological matrices [24 – 27]. Thus, poly(2-oxazoline)s are currently under intense study for biological and biomedical applications such as drug-delivery systems and for the construction of artificial cell membranes [28]. Furthermore, the possibility of structural tuning and functionalization of the polymer and the polymer termini led to the synthesis of novel amphiphilic block copolymers for micellar catalysis [29]. In other words, they are used as nanoreactors for atom transfer radical polymerization [30], metathesis [31], and the asymmetric hydrogenation of amino acid precursors [32 – 34]. The intention of the work presented here is to understand fundamental characteristics, such as the phase behavior, diffusion and aggregation of amphiphilic poly(2-oxazoline)s.

In aqueous solutions of amphiphilic diblock copolymers, spherical micelles of core-shell structure are usually formed above a certain polymer concentration, the critical micelle concentration (CMC) [4]. In a certain range of concentrations above the CMC, the micelles coexist with unimers. In polymeric amphiphiles, the CMC is typically much lower than in low molar mass surfactant systems [35]. It is therefore often outside the experimentally accessible region, and various attempts have been made to determine the CMC, for instance, by extrapolation from the micellar region using theoretical models [36] or by monitoring the fluorescence of dyes dissolving preferentially in the hydrophobic micellar core [37, 38, 39]. An additional complication in studying polymer systems is to achieve thermodynamic equilibrium, especially if the core block is long, strongly hydrophobic and/or in the glassy state. Large non-equilibrium aggregates, in addition to micelles, may be present in the solution [9, 40].

For the determination of the structures formed by amphiphilic diblock copolymers in aqueous solution, the locations of the phase transitions and for the characterization of the dynamics, a number of methods have been applied, most often in combination with each other: dynamic scanning calorimetry [41 – 43], electron microscopy [14, 39], optical microscopy [41, 44], small-angle neutron and X-ray scattering and static light scattering [18, 41 – 48], photon correlation spectroscopy and pulsed field gradient (PFG) NMR [39, 49 – 54], and dynamic mechanical spectroscopy (DMS) [55, 56]. The CMC was detected using small-angle scattering [42, 45 – 47], photon correlation spectroscopy [52], dynamic scanning calorimetry [41, 57], and surface tension measurements [41]. However, the sample preparation may be tedious and often extensive modeling of the data is required.

Fluorescence correlation spectroscopy (FCS) allows measurements of the diffusion of fluorescence labeled molecules, aggregates, and particles through a detection volume of approximately 1 fl (femtoliter) (1 μm^3) by means of confocal optics and a single-photon detector [58 – 62]. The concentration of labeled molecules can be very low (nmol/l to μmol/l), such that the detection volume contains only a few labeled molecules simultaneously. In this way, the diffusion of single (block co-)polymers through a matrix of a solution of unlabeled (ideally otherwise identical) polymers can be monitored and analyzed. Furthermore, only small sample amounts are necessary (∼50 μl). Up to now, FCS has mainly been

used for studying the interactions and the binding between biological macromolecules [61, 62], e.g., protein aggregation [63], or the formation of protein-DNA complexes [64].

Until now, only a few FCS studies of synthetic macromolecular systems have been reported. The micellization of diblock copolymers having one ionic block was investigated by adding a poorly water-soluble fluorescence agent to the solution [39]. Its solubility in the micellar core enabled the detection of the micelles, the determination of their hydrodynamic radius and to determine the (very low) CMC [39]. The diffusion of fluorescence-labeled PEO polymers at the air-water interface was studied as well [65]. In a study on so-called *Janus* micelles, which were formed in the solid phase and dissolved, their CMC in selective solvent was determined using FCS [66].

In our present study on the micelle formation in poly[(2-methyl-2-oxazoline)-*b*-(2-*n*-nonyl-2-oxazoline)] diblock copolymers, the fluorescence label is chemically attached to the diblock copolymer under study. The fluorescence-labeled polymers were used as tracers in aqueous solutions of non-labeled, but otherwise chemically identical diblock copolymers. In this way, the influence of the fluorescence label on the aggregation behavior could be minimized. By comparing with results from PCS on solutions of non-labeled polymers, we could determine the influence of the rather bulky fluorescence label on the micellization and characterize the aggregation behavior in dependence of temperature.

Experimental

Synthesis

Instruments and methods

^{1}H-NMR spectra were measured on a *Bruker* ARX 300 at 300.13 MHz. Analytical gel permeation chromatography (GPC) was carried out on a Waters 510, column 10, 50 nm, with eluent $CHCl_3$. FTIR-spectroscopy was carried out on a *Bruker* IFS 55s at 2 cm^{-1} spectral resolution (polymer films on KBr single crystals, transmission mode).

Materials

2-n-Nonyl-2-oxazoline was a kind gift from *Henkel* KGaA, Düsseldorf, Germany. All other chemicals were purchased from *Sigma-Aldrich*. Monomers and solvents were refluxed over CaH_2 for 4 h, distilled and stored under dry N_2. Piperazine was distilled and kept under dry N_2. Purification procedures for solvents and chemicals used for the cationic polymerization were performed as previously published [29, 67].

Polymerization

All polymerizations were carried out under inert conditions (Schlenk) as previously reported [29, 67].

Poly(2-methyl-2-oxazoline)$_{26}$; **PMOx$_{26}$** To a solution of 0.124 g (0.76 mmol) methyltriflate in acetonitrile (20 ml), 2-methyl-2-oxazoline (1.924 g, 22.6 mmol for $n = 30$) was added at 0 °C. The reaction mixture was stirred at 80 °C for 24 h. At 0 °C, piperazine (1.29 g, 15.1 mmol, 20 eq.) in 2 ml chloroform was added as the termination reagent and the solution was stirred overnight. After removal of the solvent and remaining excess of piperazine, the solid residue was dissolved in 15 ml chloroform, and 1 g of potassium carbonate was added. The mixture was stirred overnight. After filtration, the polymer was purified by reprecipitation (diethyl ether). The obtained polymer was isolated by filtration (using a pressure filter setup by *Sartorius*) and freeze dried (benzene). Yield: 87%

^{1}H-NMR ($CDCl_3$): δ in ppm: 3.41 (s, 104 H, -N-C**H$_2$**-C**H$_2$**-N-), 2.99 (bs, 3 H, -C**H$_3$**), 2.90 (bs, 4 H, -N-(**CH$_2$**)$_2^{piperazine}$), 2.47 (bs, 4 H, -(**CH$_2$**)$_2^{piperazine}$-NH) 2.05 (bs, 78 H, -CO-C**H$_3$**). Polydispersity index (PDI): 1.21 (from GPC); $\bar{M}_n$: 2313 g/mol (as determined by end-group analysis from NMR data).

Poly[(2-methyl-2-oxazoline)$_{40}$-b-(2-n-nonyl-2-oxazoline)$_7$]; **P[MOx)$_{40}$(NOx)$_7$]** To a solution of 0.128 g (0.78 mmol) methyltriflate in a mixture of acetonitrile (12 ml) and chlorobenzene (6 ml), 2-methyl-2-oxazoline (1.990 g, 23.38 mmol for $n = 30$) was added at 0 °C. The reaction mixture was stirred at 80 °C for 24 h. At 0 °C, 2-*n*-nonyl-2-oxazoline (0.929 g, 4.71 mmol for m = 6) was added. The solution was stirred for another 24 h at 80 °C. At 0 °C, piperazine (1.33 g, 15.6 mmol, 20 eq.) in 2 ml chloroform was added as the termination reagent, and the solution was stirred overnight. After removal of the solvent and remaining excess of piperazine, the solid residue was dissolved in 15 ml chloroform, and 1 g of potassium carbonate was added. The mixture was stirred overnight. Isolation and purification was performed as described above. Yield: 89%

^{1}H-NMR ($CDCl_3$): δ in ppm: 3.41 (s, 188 H, -N-C**H$_2$**-C**H$_2$**-N-), 3.01 (bs, 3 H, -C**H$_3$**), 2.29 (bs, 14 H, -CO-C**H$_2$**-), 2.07 (bs, 120 H, -CO-C**H$_3$**), 1.55 (m, 14 H,-CO-CH$_2$-C**H$_2$**-), 1.22 (m, 84 H, -CH$_2$-(**CH$_2$**)$_6$-CH$_3$), 0.83 (t, 21 H, -CH$_2$-(CH$_2$)$_6$-C**H$_3$**). PDI: 1.20 (GPC); $\bar{M}_n$: 4034 g/mol (NMR).

Poly[(2-n-nonyl-2-oxazoline)$_{10}$-b-(2-methyl-2-oxazoline)$_{32}$]; **P[NOx)$_{10}$(MOx)$_{32}$]** The polymerization was performed as above. To a solution of 0.067 g

(0.41 mmol) methyltriflate in 12 ml acetonitrile and 6 ml chlorobenzene 2-*n*-nonyl-2-oxazoline (0.565 g, 2.86 mmol for $n = 7$) was added at 0 °C. The reaction mixture was stirred at 80 °C for 24 h. At 0 °C, 2-methyl-2-oxazoline (1.394 g, 16.38 mmol for m = 40) was added. For the termination, piperazine (0.7 g, 8.2 mmol, 20 eq.) in 1.5 ml chloroform was used. Isolation and purification was performed as described above. Yield: 96%.

^{1}H-NMR ($CDCl_3$): δ in ppm: 3.35 (s, 168 H, -N-C**H$_2$**-C**H$_2$**-N-), 2.91 (bs, 3 H, -C**H$_3$**), 2.21 (bs, 20 H, -CO-C**H$_2$**-), 1.99 (bs, 96 H, -CO-C**H$_3$**), 1.48 (m, 20 H,-CO-CH$_2$-C**H$_2$**-), 1.15 (m, 120 H, -CH$_2$-(C**H$_2$**)$_6$-CH$_3$), 0.76 (t, 30 H, -CH$_2$-(CH$_2$)$_6$-C**H$_3$**). PDI: 1.07 (GPC); $\bar{M}_n$: 4796 g/mol (NMR).

Fluorescence labeling

PMOx$_{26}$-TRITC, P[(MOx)$_{40}$(NOx$_7$)]-TRITC and P[(NOx)$_{10}$(MOx)$_{32}$]-TRITC: Fractions of the polymers **PMOx$_{26}$**, **P[(MOx)$_{40}$(NOx$_7$)]**and **P[(NOx)$_{10}$(MOx)$_{32}$]** were taken to prepare the respective fluorescence labeled polymers of identical mass distribution and polymer composition.

In each case, 50 mg of the polymer was dissolved in 2 ml dry methanol. Then, 13 mg (0.029, 1.3 eq.) of tetramethyl rhodamine isothiocyanate (TRITC) for-**PMOx$_{26}$**, 7 mg (0.016 mmol, 1.3 eq.) TRITC for**P[(MOx)$_{40}$(NOx)$_7$]** and 5.5 mg (0.012 mmol, 1.3 eq.) TRITC for**P[(NOx)$_{10}$(MOx)$_{32}$]** were added. The solutions were stirred for three days under inert conditions and under exclusion of light. The solutions were concentrated and purified by chromatography (*Sephadex* G-25, 10 cm, methanol). The dark red fraction was isolated and dried. After characterization (chromatography, NMR and FTIR spectroscopy), the fluorescence labeling via formation of a thiourea bond was found to be quantitative.

Photon correlation spectroscopy (dynamic light scattering)

Photon correlation spectroscopy (PCS) experiments were conducted at the Institute of Macromolecular Chemistry in Prague. Dust-free solutions of the non-labeled polymers were prepared by dissolving the polymers in distilled water and by filtering the solutions into the previously de-dusted scattering cells and were sealed at room temperature. Temperature-resolved PCS measurements were performed in polarized geometry using an ALV-5000/E logarithmic correlator together with a goniometer with an index-matching vat filled with decalin. The light source was a HeNe laser operated at 632 nm. The scattered light was detected using APD detectors working in pseudo cross-correlation mode to which the signal was fed by optical fibers with a beam splitter in order to avoid artifacts in the early time regime of the correlation function. The measuring times were 30 min with 30 min waiting time. Angle-dependent PCS was performed using an ALV-setup with an ALV-6000 correlator in the cross-correlation mode, again using two detectors and a 632 nm HeNe laser.

The correlation functions were analyzed by numerical inverse Laplace transformation using the REPES program [68], which calculates the distribution of relaxation times,$A(\tau)$, from the measured intensity autocorrelation function,$g^2(t)$. From the centers of gravity of the peaks in $A(\tau)$, the diffusion coefficient is obtained using

$$D_{PCS} = \frac{\Gamma}{q^2} \tag{1}$$

where Γ is the relaxation rate ($\Gamma = \tau^{-1}$) and q the modulus of the scattering vector at angle θ, given by $q = 4\pi n \sin(\theta/2)/\lambda$,with n the refractive index of the sample and λ the wave length of the laser light in vacuum. The hydrodynamic radius,r_H, is calculated using the Stokes-Einstein equation:

$$r_H = \frac{k_B T}{6\pi\eta D_{PCS}} \tag{2}$$

where k_B is Boltzmann's constant, T the absolute temperature, and η the temperature-dependent viscosity of water included in the GENDIST program [69] used for analysis.

Fluorescence correlation spectroscopy

Fluorescence correlation spectroscopy (FCS) experiments were conducted at Fakultät für Biowissenschaften, Pharmazie und Psychologie, Universität Leipzig. Measurements could only be performed at room temperature. A stock solution of the labeled polymers (10^{-4} mol/l) was produced by dissolving the polymers in deionized and filtered water, leaving the solutions for one week in a laboratory shaker. Two protocols were followed to prepare sample solutions for FCS: (i) a solution of non-labeled polymers was prepared at a concentration of 10^{-2} mol/l and was diluted before mixing with a solution of fluorescence-labeled polymers in the desired ratio; (ii) a solution of non-labeled polymers (10^{-3} mol/l) was subject to heating/cooling cycles as performed for the PCS experiments (i.e., annealed) before mixing. The FCS measurements were performed shortly after mixing. Solutions prepared following protocol (ii) seem to be in equilibrium, i.e., fluorescence-labeled and non-labeled polymers were able to exchange, because FCS results from solutions which had been left to stand at room temperature for three days or heated to

40 °C for 24 h before the measurement were indistinguishable.

A ConfoCor 2 from *Carl Zeiss Jena* GmbH was used together with a HeNe laser ($\lambda = 543$ nm), a pinhole with a diameter of 80 μm, a BP 560–615 emission filter, and an HFT 543 plate beam splitter. The autocorrelation functions of the fluctuations of the fluorescence intensity, $G(\tau)$, were analyzed by fitting the following expression [70]:

$$G(\tau) = 1 + \frac{1}{N}\left(\frac{T_T}{1-T_T}\exp\left(-\tau/\tau_T\right)\right)\sum_{i=1}^{n}\frac{\rho_i}{\left(1+\frac{\tau}{\tau_{D,i}}\right)\sqrt{1+\frac{\tau}{\tau_{D,i}S^2}}} \quad (3)$$

where N is the total number of fluorescent particles in the observation volume, n the number of different fluorescent species, $\tau_{D,i}$ the diffusion time of the i-th species, ρ_i the amplitude of the i-th species, $S$the axial ratio of the observation volume given by $S = z_0/w_0$ with z_0, and w_0 the half-height and half-width of the observation volume, respectively. T_T is the triplet fraction, and τ_T the triplet time. w_0 was determined before each session by measuring the diffusion time of Rhodamine 6G (*Sigma-Aldrich*, $D_{Rh6G} = 2.8\times10^{-10}$ m^{2}s^{-1}, [59]), $\tau_{D,Rh6G}$. w_0 is determined from its diffusion time, $\tau_{D,Rh6G}$, by using $w_0 = \sqrt{4D_{Rh6G}\tau_{D,Rh6G}}$. w_o was usually ~0.3 μm.

Results and discussion

Characterization after synthesis

The polymerization reactions were carried out according to Scheme 1a [29, 71]. For the preparation of **P[(MOx)$_{40}$(NOx)$_7$]**, 2-methyl-2-oxazoline was used to synthesize the hydrophilic block of the polymer, for the addition of the hydrophobic block, 2-nonyl-2-oxazoline was added consecutively. Quantitative termination of the living polymerization by an excess of piperazine introduced a free secondary amine group at the polymer terminus for polymer analogous fluorescence labeling with TRITC [72]. Hence, the fluorescence label is chemically attached to the diblock copolymer. This allows for the simultaneous detection of single molecules and their aggregates by FCS. ^{1}H-NMR spectroscopy and GPC measurements showed that, under the used reaction conditions, only single termination occurred. For the second block copolymer, **P[(NOx)$_{10}$(MOx)$_{32}$]**, the synthesis sequence, 2-nonyl-2-oxazoline and 2-methyl-2-oxazoline, was reversed. By this, two comparable amphiphilic block copolymers were obtained which could be functionalized either on the hydrophilic or hydrophobic sequence (Scheme 1b). The block copolymers were characterized by means of NMR and GPC. The results are summarized in Table 1.

The yield of the fluorescence labeling was determined by chromatography, FTIR, and ^{1}H-NMR spectroscopy. The reaction of the isothiocyanate group of the fluorescence label with the secondary amino group of the polymer was found to be quantitative. The successful formation of the thiourea link between the polymer and the label was indicated by the appearance of the characteristic C = S stretching mode at 1187 cm^{-1}, whereas the characteristic mode of the arylic thioisocyanate of the free dye at 2150 cm^{-1}disappeared. Besides the quantitative and easy coupling reaction of the label TRITC and the polymer, the label was specifically selected due to its suitable excitation ($\lambda = 544$ nm) and emission wavelength ($\lambda = 572$ nm), short triplet lifetime, good photostability, minimal sterical needs as compared to other suitable labels and its relatively good water solubility (inner salt). For the present study, the last argument is of importance, since most fluorescent labels are hydrophobic and thus strongly influence the aggregation behavior of the amphiphiles under study.

Temperature behavior of the solubilization

In temperature-dependent PCS measurements between 12 and 100 °C, possible non-equilibrium states were detected. With both diblock copolymers, the PCS count rate decreases significantly during the first heating cycle above ~40 °C (Fig. 1a). This may be attributed to a decrease in the average particle size, since the count rate increases with the mass and the concentration of the scattering objects. During subsequent cooling and heating cycles, the count rate remains unchanged at a low level (Fig. 1a).

The hydrodynamic radius of the aggregates in a solution of P[(NOx)$_{10}$(MOx)$_{32}$] (averaged over the entire peak, Fig. 2a) decreases from ~90 nm at 15 °C to ~12 nm at 100 °C and remains at that value during subsequent cooling and heating (Fig. 1b). The fact that the peak is narrow (Fig. 2b) together with the linear dependence of Γ on q^2 (inset of Fig. 1b) measured at room temperature after the first heating and cooling, point to the presence of a single species only. The diffusion coefficient determined from the slope is $D_{PCS} = (2.25 \pm 0.05)\times10^{-11}$ m^{2}s^{-1}, which corresponds to a hydrodynamic radius $r_H = (10.8 \pm 0.2)$ nm. The broadness of the distribution before the first heating (Fig. 2a) together with the fact that the dependence of Γ on q^2 is not linear (not shown), indicate the presence of particles of different size. Keeping the temperature at 40 °C, even after 24 h, the count rate did not reach equilibrium. Only at significantly higher temperatures (at least 80 °C), equilibrium was reached in reasonable time.

Scheme 1 **a** Reaction scheme for the preparation of end-functionalized amphiphilic diblock copolymers. **b** Polymer analogous fluorescence labeling with tetramethyl rhodamine isothiocyanate (TRITC)

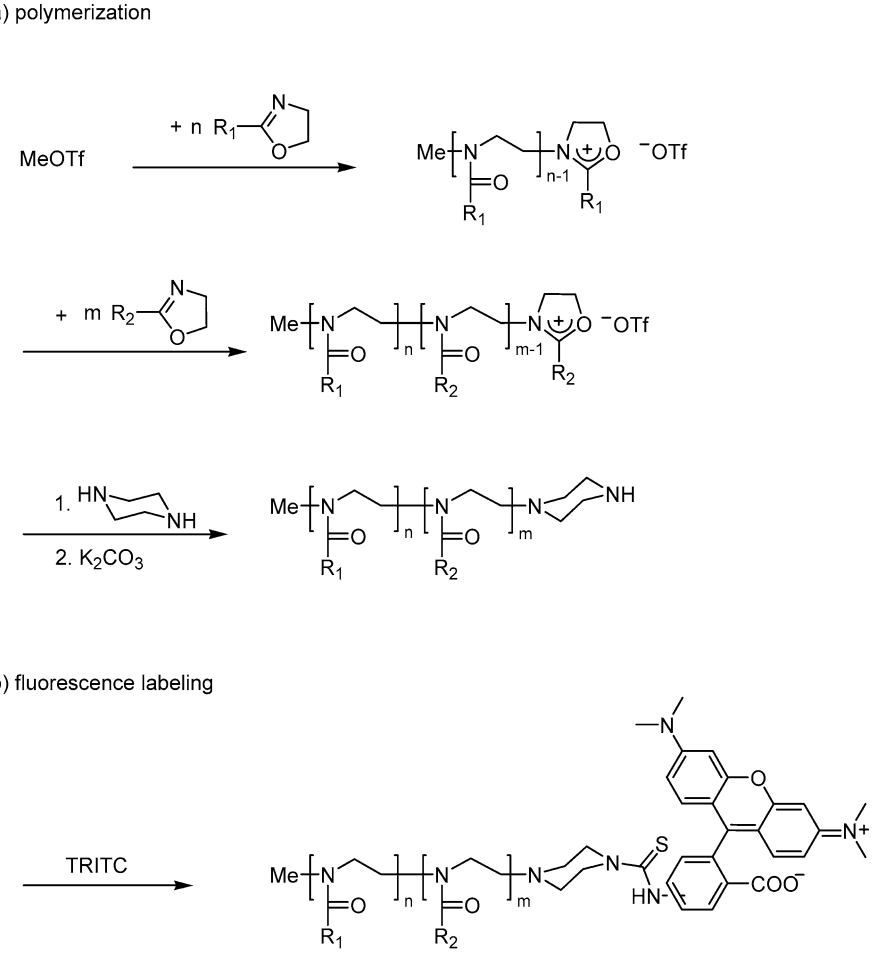

P[MOx$_{40}$(NOx)$_7$]: R_1 = Me, R_2 = *n*-Nonyl

P[NOx)$_{10}$(MOx)$_{32}$]: R_1= *n*-Nonyl, R_2 = Me

PMOx$_{26}$: R_1= Me, no second monomer

Table 1 Polymer analytical values of the polymers

Polymer	DP_n $[M1]_0/[I]_0$ 1st block[a]	DP_n $[M2]_0/[I]_0$ 2nd block[a]	DP 1st block[b]	DP 2nd block[b]	M_n ^{1}H-NMR[c]	Yield/%[d]	PDI[e]
P[$(MOx)_{40}(NOx)_7$]	30	6	40	7	4034	89	1.20
P[$(NOx)_{10}(MOx)_{32}$]	7	40	10	32	4796	96	1.07
$PMOX_{26}$	30	-	26	-	2313	87	2.21

[a]Degree of polymerization (DP_n) calculated from initial monomer/initiator feed
[b]Degree of polymerization calculated from ^{1}H-NMR spectra (from end group analysis)
[c]Molar mass ftom ^{1}H-NMR spectra
[d]Yield vs initial monomer feed
[e]Polydispersity index (PDI: $\bar{M}_w/\bar{M}_n$) as measured by GPC

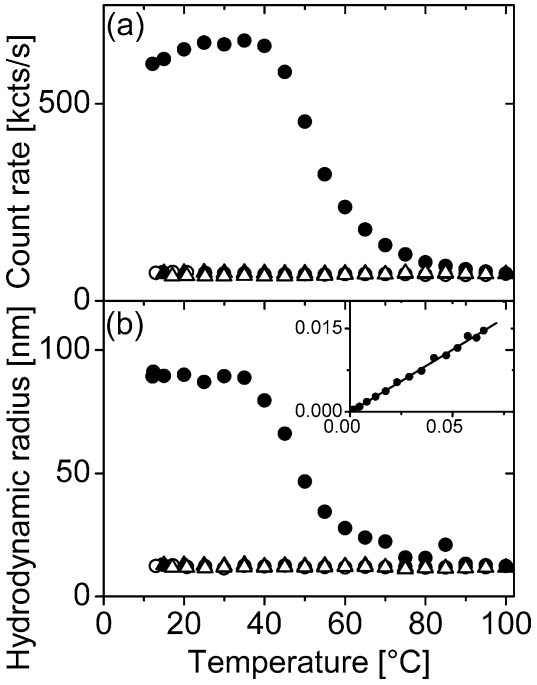

Fig. 1a,b Temperature-dependent PCS on solutions of **P[(NOx)$_{10}$(MOx)$_{32}$]**c = 3×10^{-3} mol/l: **a** count rate, (*filled circles*) first heating, (*open circles*) first cooling, (*filled triangles*) second heating, (*open triangles*) second cooling; **b** hydrodynamic radius, same symbols as in a. The *inset* shows the relaxation rate of the decay observed in the intensity autocorrelation function, Γ[μs^{-1}], in dependence of the square of the scattering vector, q^2[nm^{-2}], measured at 25 °C after the first heating. The line is a fit of Eq. (1)

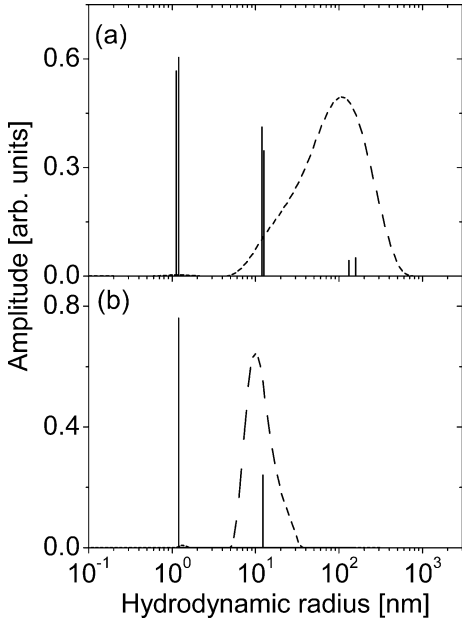

Fig. 2a,b Comparison of distributions of r_H from PCS and FCS on **P[(NOx)$_{10}$(MOx)$_{32}$]**: **a** PCS distribution of hydrodynamic radii of a solution of non-labeled polymers with a concentration $c_{nl} = 7\times10^{-3}$ mol/l prepared at room temperature and measured at 25 °C (*dashed line*). FCS-measurements from solutions with a concentration of fluorescent polymers $c_{fl} = 8\times10^{-8}$ md/l and non-labeled polymers $c_{nl} = 9\times10^{-3}$ mol/l, prepared following protocol (i) and measured at room temperature (*solid lines*). A three-component decay ($n = 3$ in Eq. 3) together with a triplet decay was fitted to the FCS correlation functions; **b** PCS distribution of a solution with $c_{nl} = 7\times10^{-3}$ mol/l (*dashed line*), after annealing. FCS results from a solution with $c_{fl} = 5.8\times10^{-8}$ mol/l and $c_{nl} = 2\times10^{-3}$ mol/l, prepared following protocol (ii) (*solid line*). A two-component decay ($n = 2$ in Eq. 3) together with a triplet decay was fitted to the FCS correlation function

The hydrodynamic radii for five different concentrations between 10^{-4} and 10^{-2} mol/l averaged over all temperatures after annealing are shown in Fig. 3. The light scattering signal of the solution of $c = 10^{-4}$ mol/l is at the detection limit, leading to significant scatter in the data. The equilibrium values of the hydrodynamic radii do not show any dependence on concentration and have values between 11 and 12 nm with an average value of (11.5 ± 0.9) nm.

All these results indicate that, during the first annealing step, large aggregates dissolve into equilibrium micelles. It has previously been observed that large and metastable aggregates form upon dissolution at room temperature and vanish upon heating [73]. The underlying processes are still unclear. Munk et al. [74] proposed that both the solid state morphology and the interactions of the two blocks with the solvent play a role. In particular, if the core (hydrophobic) block is in the glassy state, equilibration may be very slow [9]. In our system, the formation of large aggregates upon dissolution at room temperature for such relatively short poly(2-*n*-nonyl-2-oxazoline) blocks may be attributed to their crystallinity below ~150 °C [75, 76], alkyl side chain crystallization, or the existence of complex metastable aggregates of the polysoaps.

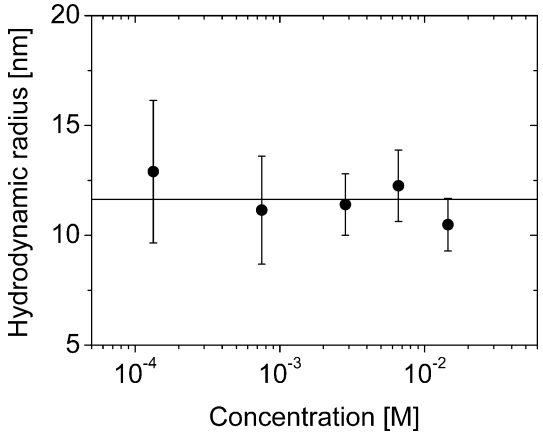

Fig. 3 Average hydrodynamic radii from PCS as a function of polymer concentration for non-labeled P[$(NOx)_{10}(MOx)_{32}$]. Averaging was performed over the first cooling and the second heating/cooling. The line indicates the average hydrodynamic radius of (11.5 ± 0.9) nm

Self-diffusional studies using fluorescence correlation spectroscopy

In contrast to PCS, FCS allows the study of samples at significantly lower concentrations. In particular, the hydrodynamic radius of the aggregates along with unimers as well as the CMC can be measured. The influence of the rather bulky fluorescence label on the aggregation behavior can also be characterized.

The two methods differ in the way diffusing particles are detected: In PCS, the scattered intensity is proportional to the particle mass and concentration, i.e., it is difficult if not impossible to detect small particles (e.g., unimers) in the presence of larger particles (e.g., micelles). In FCS, on the other hand, the fluorescence intensity of particles diffusing through the observation volume is monitored with the intensity being independent of the particle size, thus enabling the simultaneous detection of unimers, micelles, and large aggregates.

The concentration range of fluorescent particles that can be studied in FCS is rather limited: the concentration has to be high enough to obtain a significant fluorescence signal. However, the detector saturates at a certain count rate. In order to overcome this problem, solutions of polymers that were not fluorescence-labeled, but otherwise identical (**P[(NOx)$_{10}$(MOx)$_{32}$]**), were added to dilute solutions of fluorescence-labeled polymers (**P[(NOx)$_{10}$(MOx)$_{32}$]-TRITC**). The concentration of the latter was kept below 6×10^{-7} mol/l, i.e., they served as tracer molecules.

With our current FCS setup, only measurements at room temperature are possible. Therefore, our observations from temperature-dependent PCS were taken into account in order to study the amphiphilic systems in the equilibrium state. The FCS correlation functions from solutions of**P[(NOx)$_{10}$(MOx)$_{32}$]**/**P[(NOx)$_{10}$(MOx)$_{32}$]-TRITC**are compiled in Fig. 4.

Unimer diffusion at low concentration

The correlation function of a sample containing only labeled polymer (**P[(NOx)$_{10}$(MOx)$_{32}$]-TRITC**) with $c_{fl}=2\times10^{-8}$ mol/l is in good agreement with the diffusion of a single species (i.e., $n=1$ in Eq. 3) with $D_{FCS}=(1.9\pm0.1)\times10^{-10}$ m^{2}s^{-1}, corresponding to $r_H=(1.3\pm0.1)$ nm (Fig. 4a). This value is much smaller than the micellar hydrodynamic radius identified with PCS on solutions with higher concentrations (11.5 nm) and of the same order of magnitude as the estimated radius of gyration (2.3 nm) [77]. We conclude that the observed decay originates from the diffusion of individual macromolecules (unimers). In addition to this diffusional decay, a triplet decay is observed at shorter times having a triplet time $\tau_T=0.005$–0.01 ms and a triplet fraction $T_T=0.05$–0.15. The triplet time is significantly smaller than the diffusion time (τ_D between 35 and a few hundred μs), and the triplet fraction is low. The triplet decay thus does not overlap significantly with the diffusional decay.

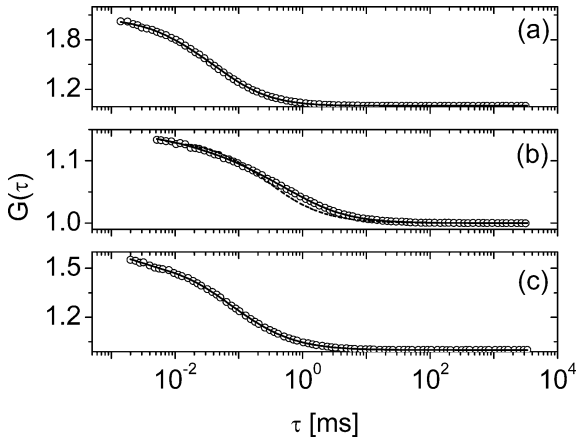

Fig. 4a–c Correlation functions from FCS for solutions of P[(NOx)$_{10}$(MOx)$_{32}$]: **a** solution of fluorescence-labeled polymers with $c_{fl}=2\times10^{-8}$ mol/l. The line is a fit to Eq. (3) with $n=1$; **b** solution with $c_{fl}=8\times10^{-8}$ mol/l and $c_{nl}=9\times10^{-3}$ mol/l, prepared and measured at room temperature. The full line is a fit of Eq. (3) with $n=3$. The dashed line is a fit of Eq. (3) with $n=2$ and using the r_H-values from PCS; **c** solution with $c_{fl}=5.8\times10^{-8}$ mol/l and $c_{nl}=2\times10^{-3}$ mol/l (annealed). The line is a fit of Eq. (3) with $n=2$

Unimers, micelles and large, metastable aggregates in solutions of higher concentration prepared at room temperature

Increasing the total polymer concentration by adding solutions of non-labeled polymers (following protocol (i)) has a pronounced effect on the correlation function (Fig. 4b): For instance, the correlation function of a solution with a total concentration of $c=9\times10^{-3}$ mol/l shows additional slower decays. A force-fit of Eq. (3) with two diffusional decays ($n=2$) with the unimer hydrodynamic radius ($r_H=1.3$ nm, Fig. 4a) and equilibrium micelles ($r_H=11.5$ nm from PCS) did not give a satisfying result at high decay times (dashed line in Fig. 4b). A fit of three diffusional decays ($n=3$ in Eq. 3) with $r_H=(1.2\pm0.5)$ nm, (13 ± 2) nm, and (140 ± 20) nm describes the experimental correlation function well (full line in Fig. 4b).

In order to identify these three processes suggested by the fit of the FCS autocorrelation function, we compared the hydrodynamic radii with the distribution of hydrodynamic radii obtained in our PCS measurements on non-equilibrated solutions with a similar concentration ($c=7\times10^{-3}$ mol/l, see Fig. 2a). Good coincidence is obtained between the distribution from PCS with the middle and slow FCS decays. We thus

identify the fast, middle, and slow processes in FCS with the diffusion of unimers, equilibrium micelles and metastable aggregates. Even at relatively low concentrations of amphiphilic block copolymers, metastable aggregates are present along with unimers and micelles. The difference in the amplitudes from the two methods is due to the different ways of detection in FCS and PCS.

Unimers and micelles in annealed solutions of higher concentration

The autocorrelation functions of annealed solutions (room temperature to >40 °C and back to room temperature) show a second, slow decay apart from the diffusion of unimers (Fig. 4c), but not as broad as for the non-annealed solutions. Here, a fit of Eq. (3) with $n=2$ nicely describes the correlation function (Fig. 4c) and results in a hydrodynamic radius of $r_H=(1.3\pm0.1)$ for unimers and (12.3 ± 0.6) nm for micelles. Also the size distribution is in good agreement with the PCS results (Fig. 2b). We note that, in the limit of small polymer concentrations, the mutual diffusion micellar coefficient as determined by PCS coincides with the self-diffusion coefficient found by FCS [78].

The slowest process attributed to metastable aggregates with $r_H=(140\pm20)$ nm vanishes after annealing. This corresponds very well to the results from the above described temperature-resolved PCS measurements, which suggest that the metastable aggregates dissolve upon annealing.

The question arises whether the aggregation of the diblock copolymer is significantly disturbed by the introduction of a fluorescence label. Therefore, additional FCS measurements were performed on aqueous solutions of water-soluble poly(2-methyl-2-oxazoline) homopolymers labeled with TRITC (**$PMOx_{26}$-TRITC**) and the corresponding non-labeled polymer (**$PMOx_{26}$**). In no case and at none of the concentrations studied (total concentration was in the range 5×10^{-7} to 2×10^{-3} mol/l) were aggregates observed, and the FCS signal was entirely due to unimers. We therefore conclude that, in the diblock copolymer solutions, it is not the fluorescence label that primarily drives the aggregation, but rather the hydrophobic block.

In order to study the influence of the position of the fluorescence label at the diblock copolymer, the **$P[(MOx)_{40}(NOx)_7]$/$P[(MOx)_{40}(NOx)_7]$-TRITC**system with the label at the hydrophobic polymer end was studied. In short: no difference to the **$P[(NOx)_{10}(MOx)_{32}]$/$P[(NOx)_{10}(MOx)_{32}]$-TRITC system** described above could be detected. The hydrodynamic radii of micelles ($r_H=(11.9\pm0.7)$ nm), and unimers ($r_H=(1.4\pm0.4)$ nm) were similar, as expected from the similar block lengths and composition.

The critical micelle concentration

Figure 5 shows the concentration dependences of the hydrodynamic radii from PCS and FCS on the two polymers in annealed aqueous solution.

With **$P[(NOx)_{10}(MOx)_{32}]$**, only the diffusion of unimers was observed at concentrations below $\sim1.5\times10^{-5}$ mol/l (Fig. 5a), whereas at higher concentrations the diffusion of fluorescence-labeled unimers and micelles contribute to the correlation curve. We assign this change to the CMC. This is in good agreement with the CMCs determined for chemically different, low molar mass, non-ionic block co-polymers, which are in the range of 10^{-8} to 10^{-2} mol/l. [9, 35, 41, 79]. It is noteworthy that CMCs at such low concentrations are very difficult to detect with conventional methods. Especially for PCS, reliable data can only be detected for sample concentrations above 10^{-4} mol/l, an order of magnitude higher than the CMC determined by FCS in this study. Again, comparing the data of our systems with different positions of the label, it is seen that the results are very similar (Fig. 5b). The results from FCS and PCS are given in Table 2.

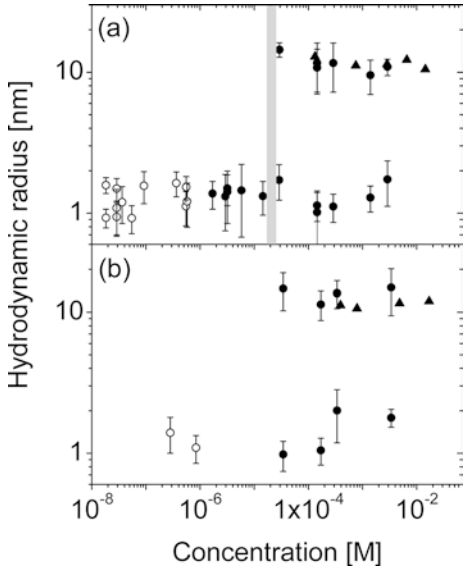

Fig. 5a,b Hydrodynamic radii found with PCS and FCS vs polymer concentration: **a $P[(NOx)_{10}(MOx)_{32}]$**: (*filled triangles*) PCS on solutions containing only non-labeled polymers. (*open circles*) FCS on solutions containing only labeled polymers, (*filled circles*) FCS on solutions containing both fluorescence-labeled and non-labeled polymers with $c_{fl}=6\times10^{-8}$ mol/l in all samples. The solutions of non-labeled polymers had been annealed. The *gray bar* indicates the CMC; **b $P[(NOx)_7(MOx)_{40}]$**. Same symbols as in a. The solutions of non-labeled polymers had been annealed

Table 2 Hydrodynamic radii from FCS and PCS averaged over all concentrations studied and critical micelle concentration

Polymer	$r_{H,\ \text{unimer}}$ [nm] FCS	$r_{H,\ \text{micelle}}$ [nm] FCS	$r_{H,\ micelle}$ [nm] PCS	CMC [M] FCS
$P[(MOx)_{40}(NOx)_7]$	1.4 ± 0.4	13 ± 2	11.9 ± 0.7	-
$P[(NOx)_{10}(NOx)_{32}]$	1.3 ± 0.2	11.3 ± 0.9	11.5 ± 0.9	2×10^{-5}
$PMOX_{26}$	1.0 ± 0.2	-	-	-

Conclusion

FCS proved to be an efficient method to study the aggregation behavior of fluorescence-labeled polymers in aqueous solution by measuring their self-diffusion coefficients. This method is fast and allows measurements at much lower concentrations than many traditionally used methods. Using polymers with a covalently bonded fluorescence label, the hydrodynamic radii of the unimers and the micelles could be determined simultaneously. Furthermore, the CMC could be determined. The micellar hydrodynamic radii are in excellent agreement with those measured by PCS. Thus, FCS is ideally suited for the study of the self-organization of non-ionic polymeric amphiphiles and polysoaps over a broad range of concentrations.

The small detection volume and the much higher time resolution of FCS allow for spatially and time-resolved measurements. For instance, different locations in biological cells can be addressed [80]. FCS may thus be a very powerful tool in studying a variety of systems in which in situ measurements are otherwise very difficult to perform, such as the transport processes (endo- and/or exocytosis and transport mechanisms within the cells) for polymer therapeutics used in drug delivery or online tracing of polymeric amphiphiles and their micelles during emulsion/suspension polymerization.

Acknowledgements We wish to thank F. Kremer, Fakultät für Physik und Geowissenschaften, Universität Leipzig, for financial support and fruitful discussions and U. Hahn, A. Beck-Sickinger, and T. Greiner-Stöffele, Fakultät für Biowissenschaften, Pharmazie und Psychologie, Universität Leipzig, for providing the FCS instrument and for help with the measurements. We also gratefully acknowledge financial support by the Deutsche Forschungsgemeinschaft, by the European Union under a Marie Curie Training Site program (contract No. HPMT-CT-2001-00396) and by the Grant Agency of the Academy of Sciences of the Czech Republic (grant No. 4050403).

References

1. Price C (1982) Colloidal properties of block copolymers. In: Goodmann I (ed) Developments in block copolymers, vol 1. Applied Science Publishers, London, pp 39–79
2. Riess G, Hurtrez G, Bahadur P (1985) Block copolymers. In: Mark HF, Bikales NM, Overberger CG, Menges G (eds.) Encylopedia of polymer sciences and engineering, vol. 2, 2nd edn. Wiley, New York, pp 324–434
3. Piirma I (1992) Polymeric surfactants. Surfactant sciences series 42. Marcel Dekker, New York
4. Tuzar Z, Kratochvíl P (1993) Micelles of block and graft copolymers in solution. In: E. Matijević (ed.) Surface and colloid science, vol 15. Plenum Press, New York, pp 1–83
5. Alexandridis P, Hatton TA (1996) Block copolymers. Polymeric materials encyclopedia 1. CRC Press, Boca Raton, pp 743–754
6. Webber SE, Munk P, Tuzar Z (1996) Solvents and self-organization of polymer. NATO ASI series, series E: applied sciences 327.Kluwer Academic Publisher
7. Hamley IW (1998) The physics of block copolymers. Oxford Science Publications, Oxford, chap 3, p 131
8. Alexandridis P, Lindman B (eds.) (2000), Amphiphilic block copolymers: self-assembly and applications. Elsevier, Amsterdam
9. Riess G (2003) Prog Polym Sci 28:1107
10. Hillmyer MA, Bates FS (1996) Macromolecules 29:6994
11. Allgaier J, Poppe A, Willner L, Richter D (1997) Macromolecules 30:1582
12. Hajduk DA, Kossuth MB, Hillmyer MA, Bates FS (1998) J Phys Chem B 102:4269
13. Förster S, Krämer E (1999) Macromolecules 32:2783
14. Discher BM, Won YY, Ege DS, Lee JCM, Bates FS, Discher DS Hammer DA (1999) Science 284:1143
15. Förster S, Berton B, Hentze H-P, Krämer E, Antonietti M, Lindner P (2001) Macromolecules 34:4610
16. Dimova R, Seifert U, Pouligny B, Förster S, Döbereiner H-G (2002) Eur Phys J E 7:241
17. Haluska CK, Góźdź WT, Döbereiner H-G, Förster S, Gompper G (2002) Phys Rev Lett 89:238302
18. Castelletto V, Hamley IW, Holmqvist P, Rekatas C, Booth C, Grossmann JG (2001) Colloid Polym Sci 279:621
19. Litt M, Rahl F, Roldan LG (1969) J Polym Sci A-2 7:463
20. Aoi K, Okada M (1996) Prog Polym Sci 21:151
21. Kobayashi S (1990) Prog Polym Sci 15:752
22. Jordan R, Martin K, Räder HJ, Unger KK (2001) Macromolecules 38:8858
23. Kobayashi S, Uyama H (2002) J Polym Sci A Polym Chem 40:192
24. Velander WH, Madurawe RD, Subramanian A, Kumar G, Sinai-Zingde G, Riffle JS, Orthner CL (1992) Biotech Bioeng 39:1024
25. Woodle MC, Engbers CM, Zalipsky S (1994) Bioconjugate Chem 5:493
26. Lasic DD, Needham D (1995) Chem Rev 95:2601
27. Zalipsky S, Hansen CB, Oaks JM, Allen TM (1996) J Pharm Sci 85:133
28. Purrucker O, Förtig A, Jordan R, Tanaka M (2004) Chem Phys Chem 5:327
29. Persigehl P, Jordan R, Nuyken O (2000) Macromolecules 33:6977
30. Kotré T, Nuyken O, Weberskirch R (2002) Macromol Rapid Commun 23:871

31. Krause JO, Zarka MT, Anders U, Weberskirch R, Nuyken O, Buchmeiser MR (2003) Angew Chemie Int Ed 42:5965
32. Zarka MT, Nuyken O, Weberskirch R (2003) Chem Eur J 9:3228
33. Nuyken O, Weberskirch R, Kotré T, Schönfelder D, Wörndle A (2003) Polymers for micellar catalysis. In: Buchmeiser M (Ed) Polymeric materials in organic synthesis and catalysis. Wiley-VCH, Weinheim, p 277
34. Heischkel Y, Stoeckel N, Nuyken O, Jordan R (2003) PCT Int Appl. BASF Aktiengesellschaft, Germany. Wo 2003, p 32
35. Evans DF, Wennerström H (1999) The colloidal domain. Wiley-VCH, p 173–217
36. Khougaz K, Gao Z, Eisenberg A (1994) Macromolecules 27:6241
37. Nivaggioli T, Alexandridis P, Hatton TA, Yekta A, Winnik MA (1994) Langmuir 11:730
38. Procházka K, Limpouchová Z, Webber SE (1996) Block copolymer micelles. 2. Fluorimetric studies and computer modeling. In: Salamone JA (ed) Polymeric materials encyclopedia, vol 1 A-B. CRC Press, Boca Raton, pp 764–772
39. Schuch H, Klingler J, Rossmanith P, Frechen T, Gerst M, Feldthusen J, Müller AHE (2000) Macromolecules 33:1734
40. Jada A, Hurtrez G, Siffert B, Riess G (1996) Macromol Chem Phys 197:3697 and references therein
41. Wanka G, Hoffmann H, Ulbricht W (1994) Macromolecules 27:4145
42. Glatter O, Scherf G, Schillén K, Brown W (1994) Macromolecules 27:6046
43. Hecht E, Mortensen K, Hoffmann H (1995) Macromolecules 28:5465
44. Zhang K, Khan A (1995) Macromolecules 28:3807
45. Mortensen K, Brown W, Nordén B (1992) Phys Rev Lett 68:2340
46. Mortensen K (1993) J Phys IV 3:157
47. Mortensen K (1996) J Phys Condens Matter 8:A103
48. Förster S, Hermsdorf N, Böttcher C, Lindner P (2002) Macromolecules 35:4096
49. Brown W, Schillén K, Hvidt S (1992) J Phys Chem 96:6038
50. Brown W, Schillén K, Almgren M, Hvidt S, Bahadur P (1992) J Phys Chem 95:6038
51. Fleischer G (1993) J Phys Chem 97:517
52. Schillén K, Brown W, Johnsen RM (1994) Macromolecules 27:4825
53. Mortensen K, Brown W, Jørgensen E (1994) Macromolecules 27:5654
54. Scheller H, Fleischer G, Kärger J (1997) Colloid Polym Sci 275:730
55. Hvidt S, Jørgensen EB, Brown W, Schillén K (1994) J Phys Chem 98:12320
56. Nyström B, Walderhaug H (1996) J Phys Chem 100:5433
57. Hvidt S (1995) Colloids Surf 112:201
58. Elson EL, Magde D (1974) Biopolymers 13:1
59. Magde D, Elson EL, Webb WW (1974) Biopolymers 13:29
60. Webb WW (1976) Q Rev Biophys 9:49
61. Rigler R, Elson E (ed) (2000) Fluorescence correlation spectroscopy. Theory and applications. Springer, Berlin Heidelberg New York
62. Hess ST, Huang S, Heikal AA, Webb WW (2002) Biochemistry 41:697
63. Riesner D (2000) Protein aggregation associated with Alzheimer and Prion diseases. In: Rigler R, Elson E (eds) Fluorescence correlation spectroscopy. Theory and applications. Springer, Berlin Heidelberg New York, pp 225–250
64. Sevenich FW, Langowski J, Weiss V, Rippe K (1998) Nucleic Acids Res 26:1373
65. Sukhishvili SA, Chen Y, Müller JD, Gratton E, Schweizer KS, Granick S (2000) Nature 406:146
66. Erhardt R, Böker A, Zettl H, Kaya H, Pyckhout-Hintzen W, Krausch G, Abetz V, Müller AHE (2001) Macromolecules 34:1069
67. Komenda T, Jordan R (2003) Polym Prepr (Am Chem Soc Div Polym Chem) 44:986
68. Jakeš J (1995) Coll Czech Chem Commun 60:1781
69. http://www.fki.uu.se/robert.johnsen/gendist.htm
70. Widengren J, Mets Ü, Rigler R (1995) J Phys Chem 99:13368
71. Nuyken O, Maier G, Gross A, Fischer H (1996) Macromol Chem Phys 197:83
72. Aicher TD, Anderson RC, Gao J, Shetty SS, Coppola GM, Stanton JL, Knorr DC, Sperbeck DM, Brand LJ, Vinluan CC, Kaplan EL, Dragland CJ, Tomaselli HC, Islam A, Lozito RJ, Liu X, Maniara WM, Fillers WS, Del-Grande D, Walter RE, Mann WR (2000) J Med Chem 43:236
73. Stejskal J, Koňák Č, Helmstedt M, Kratochvíl P (1993) Collect Czech Chem Commun 58:2282
74. Munk P (1996) Equilibrium and non-equilibrium micelles. In: Webber SE, Munk P, Tuzar Z (eds) Solvents and self-organization of polymer. NATO, ASI series, series E: Applied sciences, vol 327. Kluwer Academic Publisher (Dordrecht), pp 19–32
75. Bassiri TG, Levy A, Litt M (1969) J Polym Sci B 43:871
76. Litt M, Rahl F, Roldan LG (1969) J Polym Sci A-2 7:463
77. Estimated using CS Chem 3D ultra 7.0.0
78. Kärger J, Fleischer G, Roland U (1998) PFG NMR studies of anomalous diffusion. In: Kärger J, Heitjans P, Haberlandt R (eds) Diffusion in condensed matter. Friedr Vieweg & Sohn, pp 144–168
79. Siqueira DF, Nunes SP, Wolf BA (1994) Macromolecules 27:4561
80. Langowski J, Wachsmuth M, Rippe K, Tewes M (2000) Biomolecular shape and interactions determined by fluorescence correlation spectroscopy. In: Frénoy J-P (ed) Energies et Forces de l'Interaction entre Macromolécules Biologiques: l'Aspect Quantitatif, vol. 2, Publications CNRS, Paris, pp 65–77